Journal Pre-proof

Innovative spectral characterisation of beached pelagic sargassum towards remote estimation of biochemical and phenotypic properties

Y.A. Fidai, C. Botelho Machado, V. Dominguez Almela, H.A. Oxenford, P.-N. Jayson-Quashigah, T. Tonon, J. Dash

Please cite this article as: Y.A. Fidai, C. Botelho Machado, V. Dominguez Almela, et al., Innovative spectral characterisation of beached pelagic sargassum towards remote estimation of biochemical and phenotypic properties, *Science of the Total Environment* (2023), https://doi.org/10.1016/j.scitotenv.2023.169789

This is a PDF file of an article that has undergone enhancements after acceptance, such as the addition of a cover page and metadata, and formatting for readability, but it is not yet the definitive version of record. This version will undergo additional copyediting, typesetting and review before it is published in its final form, but we are providing this version to give early visibility of the article. Please note that, during the production process, errors may be discovered which could affect the content, and all legal disclaimers that apply to the journal pertain.

Innovative spectral characterisation of beached pelagic sargassum towards remote estimation of

biochemical and phenotypic properties

In draft for submission to: Science of The Total Environment

Authors:

Fidai, Y.A[1,2].; Botelho Machado, C.[2]; Dominguez Almela, V[1].; Oxenford, H.A.[3]; Jayson-Quashigah P-N.[4];

Tonon, T.[2]; Dash, J.[1]

1 University of Southampton, School of Geography and Environmental sciences, Highfield Campus,

Southampton, SO17 1BJ

2 Centre for Novel Agricultural Products, Department of Biology, University of York, Wentworth

Way, York YO10 5DD

3 Centre for Resource Management and Environmental Studies (CERMES), University of West Indies,

Cave Hill Campus, Barbados, BB11000

4 Institute for Environment and Sanitation Studies (IESS), University of Ghana, Ghana, P. O. Box LG

209

Abstract:

In recent years, pelagic sargassum (*S. fluitans* and *S. natans* – henceforth sargassum) macroalgal

blooms have become more frequent and larger with higher biomass in the Tropical Atlantic region.

They have environmental and socio-economic impacts, particularly on coastal ecosystems, tourism,

fisheries and aquaculture industries, and on public health. Despite these challenges, sargassum

biomass has the potential to offer commercial opportunities in the blue economy, although, it is

reliant on key chemical and physical characteristics of the sargassum for specific use. In this study,

we aim to utilise remotely sensed spectral profiles to determine species/morphotypes at different decomposition stages and their biochemical composition to support monitoring and valorisation of sargassum. For this, we undertook dedicated field campaigns in Barbados and Ghana to collect, for the first time, in situ spectral measurements between 350 and 2500 nm using a Spectra Vista Corp (SVC) HR-1024i field spectrometer of pelagic sargassum stranded biomass. The spectral measurements were complemented by uncrewed aerial system surveys using a DJI Phantom 4 drone and a DJI P4 multispectral instrument. Using the ground and airborne datasets this research developed an operational framework for remote detection of beached sargassum; and created spectral profiles of species/morphotypes and decomposition maps to infer biochemical composition. We were able to identify some key spectral regions, including a consistent absorption feature (920 – 1080 nm) found in all of the sargassum morphotype spectral profiles; we also observed distinction between fresh and recently beached sargassum particularly around 900 – 1000 nm. This work can support pelagic sargassum management and contribute to effective utilisation of the sargassum biomass to ultimately alleviate some of the socio-economic impacts associated with this emerging environmental challenge.

1. Introduction

Pelagic sargassum[1] algal blooms and associated beach depositions are an emerging environmental challenge affecting the entire tropical Atlantic region, including the Caribbean Sea, Gulf of Mexico, and Gulf of Guinea since 2011. These blooms and beaching events (as defined by Fidai et al., 2020) have a variety of impacts on social aspects and economic activities and industries such as tourism, fisheries and aquaculture, as well as public health (Chavez et al., 2020; Solarin et al., 2014; Ramlogan et al., 2017; ANSES 2017; Resiere et al., 2018). They also have detrimental environmental effects on coastal ecosystems, water quality and beach stability (McGlathery 2001; Maurer et al., 2015; van Tussenbroek et al., 2017). The impact on these sectors is further exacerbated by accumulated sargassum that decomposes after a couple of days on the beach and produces gas, leachates and organic matter which interact with wave action, resulting in hypoxic conditions and deterioration of water quality as far as 480 m from the shore (Chavez et al., 2020; Rodriguez-Martinez et al., 2019). Rodriguez-Martinez et al. (2019) estimated that 78 faunal species died as a result of accumulated and decaying sargassum in the nearshore marine environment in Mexico in 2018, including fish, crustaceans, molluscs, echinoderms and polychaetes. Similarly, van Tussenbroek et al. (2017) found that it resulted in mortality of nearshore seagrasses and associated fauna and corals in Mexico. To enable the region, especially small islands and lower income countries, to manage the challenges of pelagic sargassum events, there is a demand to identify ways of using the biomass and develop strategies to reduce their impacts. Researchers are already suggesting that the seaweed biomass has the potential to be used for: construction blocks, biofuel, fertiliser, cosmetics and more (Desrochers et al., 2022). There are two recognised species of pelagic sargassum: S. *fluitans* and S. *natans* (Taylor 1972; Guiry and Guiry 2023), and several morphotypes for each species: S. *fluitans* III and X; S. *natans* I, II, VIII, and IX (Parr, 1939). Schell et al. (2015) showed that *S. natans* I, *S. natans* VIII and *S.*

---

[1] *S. fluitans* and *S. natans* species are referred to in shorthand as 'sargassum' (following Fidai et al., 2020).

fluitans III were found across the Sargasso Sea, Antilles Current, Eastern Caribbean and Western

Tropical Atlantic in varying proportions at each location. To reduce the negative impacts of

sargassum and by utilising it as a natural resource there is a need to: i) determine if there is any

variation in physical characteristics between species morphotypes and subsequent impacts of this on

potential uses; ii) understand how decomposition in a beach environment affects its properties for

use; iii) develop an in situ method of assessing the quality and quantity of sargassum for harvesting.

To address some of these gaps, remote sensing techniques, particularly space-borne satellite

imagery, have been used to monitor pelagic sargassum, typically in the open ocean at a coarse basin

scale resolution. For example, Wang et al. (2019) considered the 'Great Atlantic Sargassum Belt'

stretching across the Tropical Atlantic. Similarly, Gower and King (2011) examined the distribution

across the Gulf of Mexico and North Atlantic. Other studies looked at smaller but still substantial

regions of the Atlantic such as Sutton et al. (2019) and Pod et al. (2016) who focussed on the

Caribbean area. Detection algorithms such as ErisNet for Yucatan Peninsula in Mexico (Arellano-

Verdejo et al., 2019) and Sargassum Early Advisory System (SEAS) for the Texas Gulf Coast (Webster

and Linton 2013) have also been established using coarse resolution space-borne remote sensing

methods for specific regions. In addition, some studies have detected sargassum at finer resolutions.

Hu et al. (2015) used measurements from various multi-spectral satellite sensors (Moderate

Resolution Imaging Spectroradiometer or MODIS, Landsat, WorldView-2) with spatial resolutions

varying between 0.02 m and 1000 m. Similarly, Ody et al. (2019) utilised a variety of satellite sensors

with spatial resolutions ranging from 10 m to 1000 m. However, Fidai et al. (2020) noted that the

majority of publications focus on general monitoring of floating sargassum at low resolution and

very few on sargassum beaching events. So far, remote sensing methods have not been commonly

used in beach environments to monitor sargassum, with most undertaking surveys and laboratory

analysis. An example of a study that used remote sensing to monitor the beach environment is

Valentini and Baloiun (2020) who used photography from smart phones and image classification

methods to monitor the coast of Martinique and detect sargassum. Leon-Perez et al. (2023)

4

detected fresh and decomposing sargassum along the shoreline and near-shore waters of Puerto Rico using space-borne Sentinel-2 imagery supported by drone photographs. Development in access to uncrewed aerial systems (UASs) provides an opportunity for monitoring sargassum. They have been used in parallel fields such as for monitoring harmful algal blooms (Wu et al., 2019) and other beached macroalgae such as *Rugolopteryx* (Roca et al., 2022), which demonstrates there is the potential to utilise them for sargassum.

Field spectroscopy has been used to distinguish vegetation at higher resolutions. Szekielda et al. (2010) used an airborne portable hyperspectral imager to measure floating windrows. Similarly, Dierssen et al. (2015) utilised an airborne imaging spectrometer to distinguish a mass of floating sargassum and seagrass at 1 m resolution. Airborne hyperspectral and thermal infrared imagery has also been used to generate spectra of floating aggregations of submerged sargassum (Marmorino et al., 2011). This high spectral resolution monitoring and mapping technique is commonly used to characterise the reflectance of natural surfaces in a variety of environments such as forest canopies for species identification (for example, Malhovsky et al., 2019; Asner et al, 2015), and agriculture for crop health and type (for example Bian et al., 2013; Su, 2020). It has been used to discriminate benthic, subtidal, and intertidal macroalgal species as well (Casal et al., 2013; Olmedo-Masat 2020). Spectroscopy is also often used for scaling-up measurements from small areas to scenes, and even satellite sensors, as achieved by Gamon et al. (2006) on linking leaf measurements to canopy data. Applying this technique to beached sargassum deposits has the potential to contribute towards addressing current research gaps in understanding the spectral properties of sargassum and their implications for valorisation, and ultimately enhancing monitoring capacity from freely available satellite data to facilitate more appropriate management of this resource.

In this context, the focus of this research was to develop an operational framework for remote detection of beached pelagic sargassum to improve valorisation potential with the specific aims of: i)

evaluating the potential of spectral reflectance data to differentiate between species/morphotypes of pelagic sargassum (*S. fluitans* III, *S. natans* I and *S. natans* VIII); ii) exploring spectral variation in sargassum species across levels of decomposition (freshly deposited (<1 day) and recently deposited (<3 days)); iii) exploring the potential of detecting species/morphotypes and decomposition levels using 'off-the-shelf' UASs; and iv) inferring biochemical composition of sargassum species/morphotypes from spectral profiles.

2. Methods

2.1 Field Data Collection Methods

2.1.1 Study Sites

Beach surveys were undertaken at Consett Bay, a small cove in Barbados, and at Sanzule village, a long straight open beach, in the Ellembelle District of Ghana's Western Region (figure 1). In Barbados, sargassum was accumulated and densely stacked on the beach with the different morphotypes tangled together, and there was a clear difference between the freshly deposited and the decomposing sargassum (more recently termed fresh gold and old gold (Small et al., 2022)). In contrast, at Sanzule, the samples were scattered across the beach as individual thalli and not tangled together. These locations were selected as they have both experienced regular pelagic sargassum deposits on their coastlines over the past decade and these beaches support the daily employment and livelihoods of communities particularly through fishing and tourism.

Figure 1 Maps showing location of data collection sites and images of beached sargassum sampled. Basemap sources: Esri, FAO (Food and Agriculture Organization of the United Nations), USGS (United States Geological Survey), and Earthstar Geographics.

A field spectrometer (SVC HR-1024i) was used at both sites to collect ground spectral measurements. The SVC HR-1024i is a high-performance single-beam field spectroradiometer measuring over the visible to short-wave infrared wavelength range (350 - 2500 nm) with internal GPS and wireless communication capabilities. It can be used with the integrated lens held above the sample (Consett Bay), or with a contact probe (with its own light source) placed directly on the sample (Sanzule).

2.1.2 Sampling Framework

In Barbados, beach surveys were undertaken in March 2022, and in Ghana in June 2022. Two differing methods of data collection were used to accommodate for the time of day, weather, and volume of fresh sargassum deposited on each of the beaches (illustrated in figure 2).

Consett Bay beach was covered with accumulated layers of sargassum morphotypes mixed together. The survey was undertaken at low tide, shortly after sunrise, as these conditions allowed for the field spectrometer to be used directly over the samples (method 1). A longshore transect was set up and white ground markers were placed every 5 m to distinguish boundaries of fresh golden and recent brown deposits of sargassum and to identify sample points to support UAS imagery processing. The field spectrometer was held at 0.15 m directly above the target, which gave a field of view with a diameter of 0.4 m. The instrument was calibrated with a white panel at each sample site, each sample was measured five times and averaged to reduce the impact of atmospheric noise and user movement on the final results. Additional calibrations were made if there were any noticeable changes to sun/cloud cover between measurements. As the sargassum beach deposits in Barbados were entangled, the thalli were sorted by morphotype to fill a quadrat (0.4 m diameter) and measured with the field spectrometer as above to obtain profiles for each morphotype found (*S. natans* I, *S. natans* VIII and *S. fluitans* III). The DJI Phantom 4 UAS with integrated RGB camera was flown at 45 m height with 75% front and 65% side overlap to give 0.012 m image resolution, over a 70 m extent using the 'corridor' flight plan outlined in Baldwin et al. (2022).

In Sanzule, low tide took place close to sunset and the weather conditions were cloudy; this, combined with a scattering of sargassum deposits across the beach, meant it was most appropriate to use a contact probe in conjunction with the field spectrometer (method 2). Flags and ground markers were laid out at 5 m intervals across a longshore transect (similar to protocol at Consett Bay). The thallus deposited nearest to each marker was sampled by placing it in a specimen tray and measuring directly onto the sample with the contact probe; 20 measurements were taken and

averaged for each sample. Older deposits were observed on the beach, but these were likely to have been deposited >3 days previously and were not measured as they were decomposing and not 'intact' to allow sampling. Morphotype sorting was not required in Sanzule as the thalli were mostly not entangled and were measured individually along the transect, *S. fluitans* III and *S. natans* VIII were identified.

Transect set-up and drone image data collection

Species sorting

Field spectrometer (SVC HR-1024i) data collection
Method 1 (Barbados)
Wide angle measurement used where there was lots of sargassum.

Field spectrometer (SVC HR-1024i) data collection
Method 2 (Ghana)
Measurements taken with contact probe where there was limited
deposits of sargassum.

Figure 2 Flow chart and images illustrating the field conditions and the two different methods used to collect ground measurements.

2.2 Data Processing

2.2.1 Spectral Data

Spectral profiles of pelagic sargassum morphotypes S. *natans* I, S. *natans* VIII, and S. *fluitans* III were created by using a combination of software packages including 'SpectraGryph 1.2.16d', 'Microsoft Excel' and 'R version 4.2.2' (R Development Core Team, 2021) to process and analyse spectral beach survey data collected using the field spectrometer. The SVC HR-1044i model can collect each reading and via Bluetooth share it to a mobile phone to store it as a '.sig' file. This feature was used to store the data in a cloud location instantly. Later, the '.sig' files were uploaded to the SpectraGryph software, where the curves of multiple readings were averaged and exported to a '.csv' file. Next, MS Excel and R version 4.2.2 were used to explore patterns and plot the data. To evaluate the potential of ground spectral data to distinguish between species/morphotypes of pelagic sargassum (first aim of our study), and to explore spectral variation in sargassum species across levels of decomposition (second aim), two approaches were used: first, the full spectra were examined and statistical tests were performed, and second, indices were utilised to explore classification and upscaling potential. The spectral data were first explored by applying a two-way analysis of variance (ANOVA) statistical test. This was to assess the interaction effects between the reflectance of the spectral profiles grouped into 10.0 nm wavelength intervals (response variable), the three species/morphotypes and the two decomposition levels (categorical variables). The Tukey multiple comparisons of means was used to establish if the categorical variables (three species/morphotypes and the two decomposition levels) had statistically different spectral profiles by determining whether there was a difference in the means of all the possible pairs of wavelengths. This contributed to establishing whether or not they could be confidently mapped and upscaled.

The potential for biochemical estimation (fourth aim of our study) was explored by considering that the spectra were reflectance curves and the inverse of absorbance curves, and thus Curran's (1989) work on foliar biochemistry could be applied to the spectra to determine which regions of the curve

are indicative of different compounds. This was supplemented with research on chemicals we expect

to find in brown algae such as sulfates and fucoidans. Wavelengths of identified compounds were

included in creation of figure 10 as an indication of dominant absorption features (Machado et al.,

2022; Agatonovic-Kustrin et al. 2020). Similarly, knowledge of various chemicals not expected to be

seen in sargassum such as those found exclusively in red algae were also researched and the regions

of the spectra where we expected to see them were explored (Shalev et al., 2022).

Once spectral differences were established, indices were selected and applied to the data, the

reflectance values of the central wavelengths and the wavelengths ±10 were averaged to reduce any

potential noise or errors (blue 450 nm, green 550 nm, red 650 nm, near-infrared (NIR) 800 nm). The

indices selected were the normalised difference vegetation index (NDVI) (1) and the normalised

green-red difference index (NGRDI) (2). NDVI was selected as it is popular for monitoring vegetation

and algae, and it has been used at coarser resolutions to monitor sargassum (Dierssen et al., 2015;

Hodgkins et al., 2017; Hu, 2009; Hu et al. 2015). NGRDI was chosen for two reasons. Firstly, it has

been used with drone imagery to detect algae with success (Xu et al., 2018; Gao et al., 2018);

secondly, it utilises only the visible bands of the electromagnetic spectrum, allowing it to be applied

to both the ground spectral measurements and the UAS imagery data collected.

$$NDVI = \frac{NIR - Red}{NIR + Red} \qquad (1)$$

$$NGRDI = \frac{Green - Red}{Green + Red} \qquad (2)$$

In addition to the spectral indices, the absorption band depth (ABD) of the identified feature was

established. To do this, the band depth relative to the continuum was calculated following the

methods developed by Kokaly and Clark (1999). As illustrated in figure 3, first the continuum line

12

was established through applying a linear interpolation between the peaks surrounding the feature (92 - 1080 nm). Then the band depth of each point in the absorption feature was calculated by subtracting the reflectance of the actual wavelength from the linear interpolation, and then the average of the band depths was calculated to generate a final value for ABD for each spectrum.
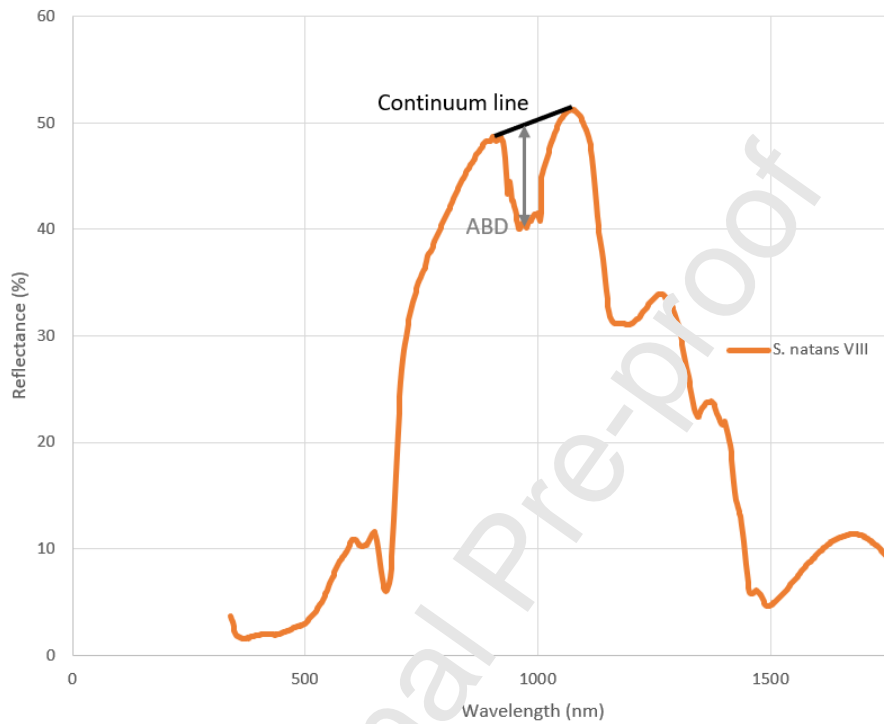

Figure 3 Illustration of how the absorption band depth (ABD) was calculated. First, the continuum line was created via application of a linear interpolation between the two peaks, and then the depth was determined by calculating the difference between the reflectance measured at each wavelength on the curve and the value on the continuum line; the band depths for all points in the feature were then averaged to give a final value.

To establish if the indices and ABD results were statistically significantly different for each species/morphotype and decomposition level, *k*-means cluster analysis was undertaken for the species and the decomposition levels. This unsupervised classification method showed if the data converged around the centroid of the cluster, meaning that the results for each of the indices were consistent for all classification categories, or if there was no statistically consistent pattern in the indices calculations.

2.2.2 UAS Data

To explore the potential of detecting and distinguishing species/morphotypes and decomposition levels using an 'off-the-shelf' UAS (third aim of our study), the images captured were processed using the 'Structure from Motion' (SfM) and 'Multi-view Stereo' (MVS) algorithms implemented in DroneDeploy (Barbados) and Agisoft Metashape (Ghana). Both applications have been reported to yield comparable results (Kloc et al., 2021; Blach et al., 2019). The SfM analyses involved, first, the alignment of the images that includes detection and matching of features, to develop the basic image structure (Mancini et al., 2013). Second, a pixel- based dense stereo reconstruction was carried out using the aligned data, and finally, orthomosaics were produced and used for further analysis. For the Ghana dataset, the geometric accuracy for the airborne image was 0.2 m root-mean-square error (RMSE), while Barbados had an RMSE of 0.3 m, both being in the acceptable range as outlined by Baldwin et al. (2022). Supervised classification was carried out on the orthomosaic using the Semi-Automatic Classification Plugin (SCP) (Congedo, 2021) in QGIS (version 3.10 A Coruña) software. Regions of interest (ROI) covering the same 0.4 m diameter sampling locations that the field spectrometer measured in Consett Bay were digitised (identifiable by ground markers in the imagery) and the spectral profiles for each class (i.e., fresh gold and recent brown deposits) were calculated. To establish if there was a statistical difference between the classes the pairwise Bray-Curtis Dissimilarity Index was calculated between the digitised ROI plots using the SCP in QGIS. This index returns a percentage between 0 and 100 where 0 indicates identical data and 100 indicates complete dissimilarity and is often used to examine dissimilarity between vegetation plots (for example Feret and Asner, 2014). Next, the regions of interest were expanded to include measurements from across the image to determine the impact of shade and other variations, and the Bray-Curtis Dissimilarity Index was re-calculated. If the Bray-Curtis Dissimilarity Index was above 90% it was considered that the profiles were statistically different, and a supervised classification could be applied to the whole image; if it was below 90% then they were considered not statistically distinct. The minimum distance method for supervised classification was applied as it has been used successfully to identify macroalgae (Olmedo-Masat 2020) and was considered simpler to implement

14

for this dataset. Next, the NGRDI was applied to the image and the range of NGRDI for each field in the classification was calculated.

3. Results and Discussion

3.1 Spectral Profiles

In figure 4 the spectral response of fresh sargassum is presented. In the visible electromagnetic range (400 - 700 nm) we observe that there is higher reflectance in the green region (500 - 600 nm), and there is more absorption in the red region (600 –700 nm). This is important as variation in the red portion is widely used as an indicator of chlorophyll abundance which can be indicative of plant health and phenological stage (Myeni et al., 1995). Along the red edge (sharp increase between red and near-infrared reflectance), there is a sharp increase in reflectance to the near-infrared region (>700 nm). The water absorption region (970 nm) is distinct where sargassum has a dip in reflectance to below 31%. The spectral profile of sargassum is largely similar to what we expect to see in typical terrestrial vegetation, indicating that existing terrestrial vegetation detection and monitoring methods are transferable for use with beached sargassum. Variation in reflectance of wavelengths can be attributed to numerous bonds characteristic of various chemical compounds as explored later (section 3.4)
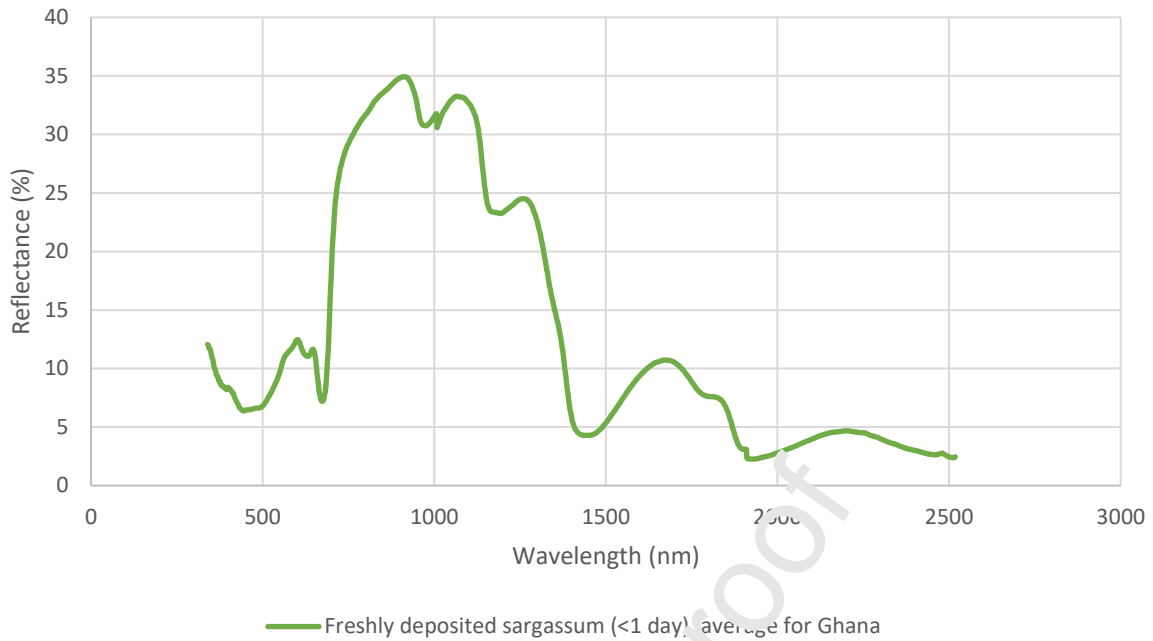
Figure 4 Spectral profile of mixed sargassum species/morphotypes (measured using method 2).

In Barbados, three morphotypes were found (*S. fluitans* III, *S. natans* I and VIII) and in Ghana, two morphotypes were found (*S. natans* VIII and *S. fluitans* III). The spectral profiles of morphotypes found in Barbados and Ghana (figure 5) have some distinctions. In the blue (400 - 500 nm) and green (500 - 600 nm) regions, all three morphotypes are alike, but in the red region *S. natans* I has a wider spectral feature than the other morphotypes. All three species show an increase in reflectance along the red-edge, but *S. natans* increases less sharply. A consistent feature observed in all the spectra was a deeper absorbance profile between 920 nm and 1080 nm, and as such, this was used to calculate the ABD. Variation in water absorption (~970 nm) can be observed in the spectral profiles between all morphotypes. In both locations *S. natans* VIII consistently has a lower reflectance (at ~970 nm), indicating increased water absorption compared to the other morphotypes. Whilst the morphotype profiles (especially *S. fluitans* III and *S. natans* VIII) are closely aligned, we theorise that the variation in absorption is a consequence of differences in biochemical composition (further explored in 3.4). We also observe that the spectral profiles from Ghana have generally lower reflectance peaks and smoother curve than Barbados above 1800 nm, and suggest that this is likely

due to variation of instrument used (i.e., contact probe use versus integrated lens) and the
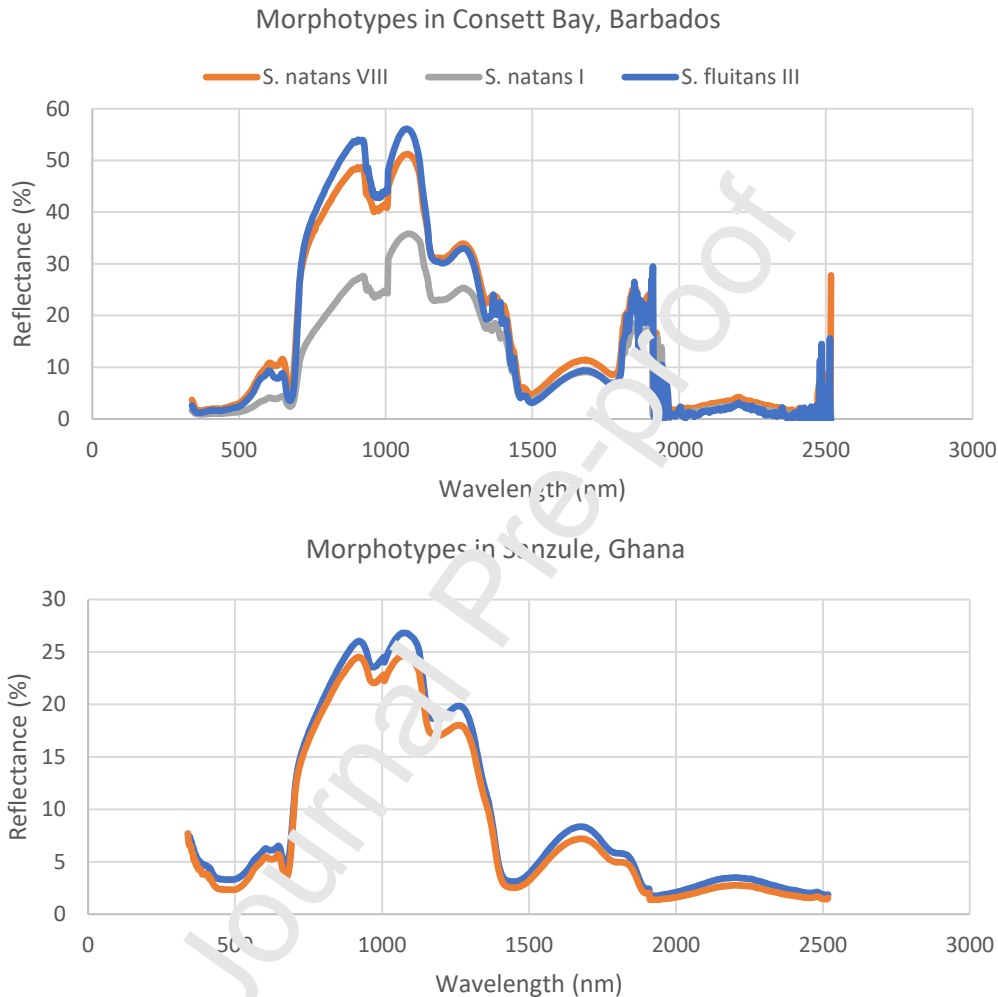
associated atmospheric interactions with method 1.

Morphotypes in Consett Bay, Barbados

Morphotypes in Sanzule, Ghana

Figure 5 Spectral profiles of sargassum morphotypes (S. natans VIII, S. natans I, S. fluitans III) found at both beach survey locations (Top: Consett Bay, Barbados; Bottom: Sanzule, Ghana).

When two-way ANOVA and Tukey multiple comparisons of means was performed on the species

spectra, the Barbados dataset shows there was a statistical difference ($F_{2, 218}$ = 9094.64, $p \leq 0.001$) in

the reflectance values of *S. natans* I when compared to the *S. natans* VIII and *S. fluitans* III ($p < 0.001$),

but *S. natans* VIII and *S. fluitans* III were not statistically different ($p = 0.87$). In Sanzule, the ANOVA

analysis shows that there was statistical difference between S. *natans* VIII and S. *fluitans* III ($F_{1, 218}$ =

11585.86, p = 0.001) indicating that the variance between species curves was not consistently statistically distinct across both locations; multiple factors such as chemical composition, thallus age, epiphyte load, extent of sun-drying on the beach, and/or atmospheric interaction (particularly for method 1), could contribute to this observed variation.

Freshly deposited and recently deposited sargassum spectral profiles display some distinct features (figure 6). In the green wavelength region (500 - 600 nm), fresh sargassum has higher reflectance, and in the red wavelength region (600 – 700 nm), fresh deposits have a narrower and deeper profile than recent deposits. Both sharply increase along the red edge. The water absorption region (970 nm) is also varied where freshly deposited sargassum has a stronger absorbance (deeper profile) than recently deposited sargassum, indicating that the recent deposits have less water and are drying on the beach, which supports our in situ observations. When comparing the decomposition spectra, the two-way ANOVA analysis confirmed that fresh and recent deposits have distinct spectral profiles (($F_{1, 218}$ = 20461.30, p ≤ 0.001). Changes in illumination might have affected reflectance, however, care was taken to remove the effects of changes in illumination by using a reference panel between measurements to normalise the spectral response and by removing the effect of solar radiation. Additionally, a standard protocol was followed for each measurement to ensure that the top canopy of beached sargassum was measured, and the accumulation was not disturbed to prevent collecting measurements from within the pile which may have been differently affected by sun drying.
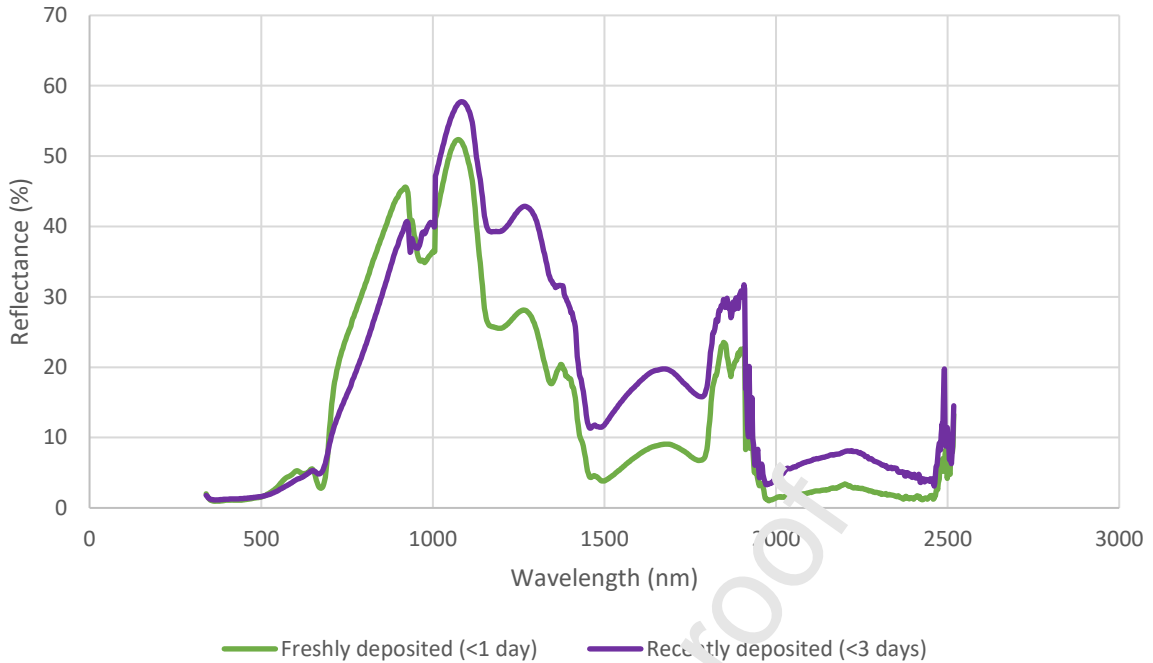
Figure 6 Spectral profiles of fresh (<1 day) and recent (<3 day) beach deposits of sargassum measured using method 1 at Consett Bay (Barbados).

3.2 Spectral Indices and Clustering Analysis

The NDVI and NGRDI, along with the ABD, were calculated for each spectral profile. As shown in table 1, recently deposited sargassum has slightly lower NDVI values than freshly deposited, which supports that they were older samples which have started to dry or decay on the beach and are less green. The ABD average values showed that there is a difference, indicating that recently deposited sargassum has a less trough between 920 and 1080 nm. Similar to NDVI, the NGRDI results show that whilst there is some overlap, the recently deposited sargassum has lower NGRDI values than freshly deposited. The results in table 1 are congruent with the results of the ANOVA analysis.

19

Table 1 Values for NDVI, NGRDI and ABD indices applied to fresh (<1 day) and recent (<3 day) beach deposits of sargassum.

		Freshly Deposited	Recently Deposited
NDVI	Min	0.67	0.55
	Max	0.76	0.72
	Mean	0.72	0.62
ABD	Min	4.21	1.68
	Max	9.63	6.45
	Mean	6.39	3.60
NGRDI	Min	-0.22	-0.25
	Max	-0.29	-0.45
	Mean	-0.25	-0.36

After the NGRDI and NDVI were plotted, *k*-means cluster analysis was undertaken. The morphotypes (for both locations) did not converge as 27% of the points were not statistically close to their cluster (figure 7); it was observed that S. *fluitans* III was most consistent with fewest samples falling outside the cluster. There is of course a notable difference in the number of samples of each morphotype, *S. fluitans* III appeared to be most common on the beach, whereas *S. natans* I was least common and was not sampled in Sanzule. In 100% of the cluster calculations, S. *natans* I was not independently clustered. The cluster analysis for both indices and the ABD indicated 18% of the samples did not converge. There is an uneven number of samples for each morphotype and additional samples, especially for *S. natans* I, would be beneficial in establishing more confident clusters. Other factors including thallus tissue condition, age and epiphyte load could also contribute to variation in the spectral profile and resultant clusters. *S. fluitans* III was the most sampled morphotype, indicating that it was the most abundant morphotype in the sargassum beaching event in Sanzule. *S. fluitans* III has been identified as the dominant morphotype in other sargassum events in the Tropical Atlantic as well, such as in Jamaica (Machado et al., 2022; Davis et al., 2021), in Barbados (Alleyne et al., 2023), and in Mexico (Garcia-Sanchez et al., 2020).

The results for the different decomposition levels showed they were more distinct with less than

17% not converging with their cluster (figure 8). When the ABD was plotted with both NDVI and

NGRDI, and the *k*-means cluster analysis was applied to both combinations, both indices did not

have converging clusters and in both cases 25% of sample points did not converge with their cluster.

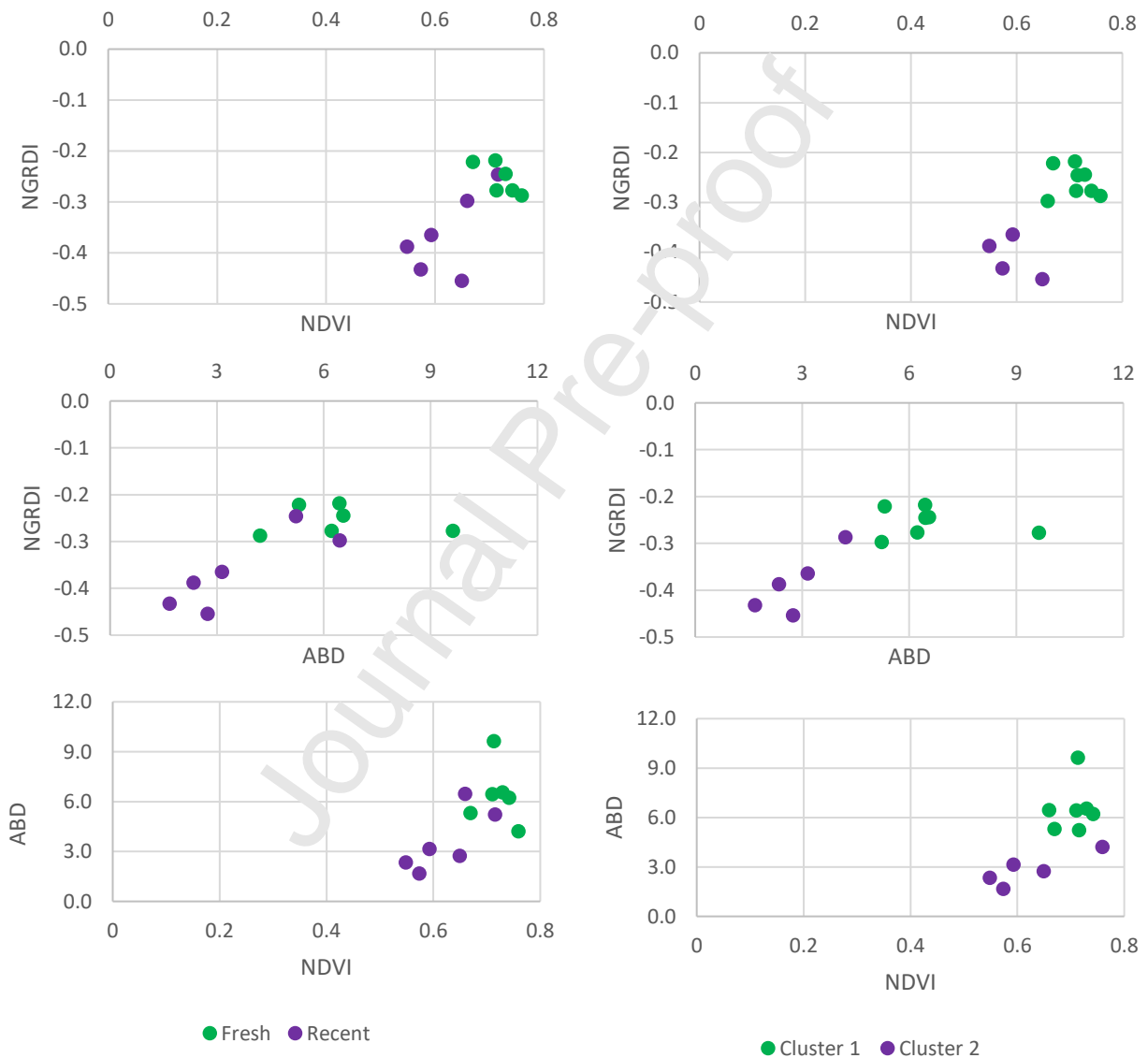Thus, it was inferred that the decomposition clusters where more distinct than the species but

maintain some overlap.

Figure 8 Cluster analysis graphs showing decomposition differentiation of mixed species in Barbados, with the decomposition clusters on the left (each point represents the calculated indices from the spectra) and the k-means cluster results on the right.

21

We theorised that some of the decomposition samples did not cluster as the measurements may have been affected by variation in sunlight due to cloud passing overhead, or by shade/shadows from vegetation along the beach. Additionally, method 1, compared to method 2, provides more opportunity for atmospheric interference as well as user error and variation. More specifically, a distance of 0.15 m to the target was measured at each sampling point to record spectra for 0.4 m sample diameter. However, over multiple recordings, the user could, due to different reasons including tiredness and/or wind, move the spectrometer closer or further from the target, changing the size of the measured area and potentially including adjacent seaweed that was outside the sample category, and this would result in erroneous data. It was not possible to use a tripod for consistency due to a lack of access to equipment that could enable measurement as low as 0.15 m height from the ground in these field conditions. For these reasons, we recommend method 2 over method 1 for measuring beached sargassum samples. Putman et al. (2023) demonstrate the success of using citizen science in monitoring coastal inundations, there is also an opportunity to use this here to expand the number of samples collected and further explore the spectral properties, for example, low-cost sensors or photography would be an accessible method of data collection to distinguish sargassum decomposition levels.

3.3 UAS Mapping

As the ANOVA statistical tests, supported by the *k*-means cluster analysis, indicated that there was variance in decomposition spectra from Consett Bay (Barbados), the potential of differentiating these in drone imagery was explored. The supervised classification of the drone imagery was achieved by digitising the same 0.4 m sample regions that were measured in situ with the field spectrometer as regions of interest for classification training data. The spectral signatures were calculated (supplementary material figure 1) and it was observed that the red region had lower reflectance values than the green, which is different to what was found in the ground measurements. As such the Bray-Curtis dissimilarity index was calculated to determine if the

digitised ROIs for recent and fresh deposits were differentiated. The Bray-Curtis result was 95.66%, indicating that they were statistically distinct, but the confusion matrix indicated an overall accuracy of 62% (supplementary material table 2) indicating that the classification accuracy was low. After classification of the images, it was observed that there were some errors in classifying sargassum shaded by vegetation, which likely contributed to the low overall accuracy. As such, the supervised classification was repeated, separating fresh deposits, recent deposits, fresh deposits with shadow/shade, and recent deposits with shadow/shade. The Bray-Curtis dissimilarity index was calculated again, and the results showed a statistical difference between fresh and recent deposits of 91.73% and the confusion matrix showed a higher and improved overall accuracy of 83.55%. It also enabled the classification map (figure 9) to closer match the identified boundary markers (white discs).

In the classification image, we observed that fresh sargassum was closer to the water and recently deposited sargassum was further from the shore, which aligned with our in situ observations. Although the overall accuracy was 83.55%, some errors distinguishing between fresh shaded and recent shaded deposits remained particularly where sargassum was deeper, creating shade over more shallow areas.

Figure 9 Supervised classification of UAS imagery. True colour RGB (top) and classification differentiating freshly and recently deposited sargassum, and shaded regions (bottom).

The NGRDI values were calculated (table 2), and it was observed that there was some overlap in the range of NGRDI for fresh and recently deposited sargassum but there were distinct averages. From these results it is evident that there is the potential for fresh and recent deposits of sargassum to be distinguished in drone imagery, and to further this analysis it would be useful to obtain drone imagery at midday to reduce the impact of shade/shadow to enable a more robust classification and confident NGRDI identification range.

Table 2 NGRDI values calculated from drone imagery classification.

	Freshly Deposited NGRDI	Recently Deposited NGRDI
Drone Imagery Supervised Classification	Min: -0.30 Max: 0.96 Mean: 0.19	Min: -0.58 Max: 0.97 Mean: 0.17

A potential extension of the operational framework would be to connect the ground based and airborne measurements. Due to various logistical reasons, including access to equipment and weather conditions, it was not possible for this to be explored (supplementary materials 1).

Remote sensing, in particular UASs, are being increasingly used to map coastal agriculture, vegetation, and habitats. For example, Nurdin et al. (2023) used drone imagery to map the spatial distribution of seaweed farming, and Diruit et al. (2022) have mapped macroalgal habitats using hyperspectral imagery. In a sargassum context, methods for high resolution coastal monitoring are being established. For example, de la Barreda-Bautista et al. (2023) have explored high spatial resolution (3 m) monitoring in Mexico. However, application in this context is new and this work contributes to its progress. Indeed, Lazcano-Hernandez et al. (2023) and Fidai et al. (2020) have highlighted the need to increase near-shore and beach monitoring of sargassum where communities experience significant impacts and prediction and management measures are needed, considering that most research to date has focussed on floating blooms.

3.4 Biochemical analysis

The biochemical analysis of sargassum (figure 10) highlights relevant chemical signals and allows us to compare decomposition and species variation. Where there is a trough, we assumed that there was an increased presence of a chemical. The region of the curve that ABD was calculated from (92-1080 nm) is also inclusive of the region where water content can be observed. The variation in depth between spectra could be explained by a difference in water content; recently deposited sargassum had been exposed to the sun and wind on the beach, begun to dry out, change colour, and its ABD was lower when compared to freshly deposited sargassum.

The interpretation of the figure is supported by biochemical analyses of Ghanaian (Rhein-Knudsen et al., 2017) and Jamaican sargassum (Machado et al., 2022), who used laboratory analytical procedures to establish the biochemical content of fresh and dried samples. Analysis of the pelagic sargassum biochemical composition showed presence of compounds such as proteins and monosaccharides, which can also be estimated from the figure. For example, we could identify various protein signals in the regions of 910 nm, 1020 nm, 1510 nm, 1690 nm, 1940 nm, 1980 nm,

25

2060 nm, 2130 nm, 2180 nm, 2240 nm, 2300 nm, 2350 nm; sugar signals (possibly monosaccharides) were present at 1445 nm, 1490 nm, 1580 nm, 1780 nm, 1960 nm, 2080 nm, 2270 nm. Hu et al. (2015) noted that sargassum has a distinctive curvature at ~630 nm due to its chlorophyll c pigments, which we also observed.

From the earlier statistical analysis, it was found that the species/morphotypes were not consistently statistically different in Barbados and Ghana, therefore we can infer that their biochemical composition is also similar. Davis et al. (2021) observed that qualitative composition of Jamaican sargassum samples was homogeneous, with differences in quantities of certain compounds between morphotypes. Using this evidence, we can suggest that the variation in spectra could also be attributed to difference in the quantities of biochemical compounds, in addition to the potential methodological and atmospheric impacts on the data collection previously mentioned.

Analysis of reflectance of pelagic sargassum could be potentially useful for compounds specific to brown algae such as mannitol, laminarin, phenolics, alginate and fucose containing sulfated polysaccharides. These chemicals are supporting the use of brown algae in a number of industrial applications and are therefore of interest for the valorisation of sargassum. From initial desk-based research, the peaks and manufacturer supplied spectra of these chemical compounds fall beyond the range of the field spectrometer used in our study, therefore a wider range of wavelength data would be required to enable reflectance detection of these chemicals. Importantly, whilst there is a goal to valorise sargassum and understanding the biochemical composition works towards this, there are constraints and challenges associated with valorisation. These are summarised by Oxenford et al. (2021) who note that the supply of sargassum is unpredictable and variable; the chemical composition is variable and can have micro-pollutants; and there are difficulties surrounding harvesting, transport and storage of sargassum.
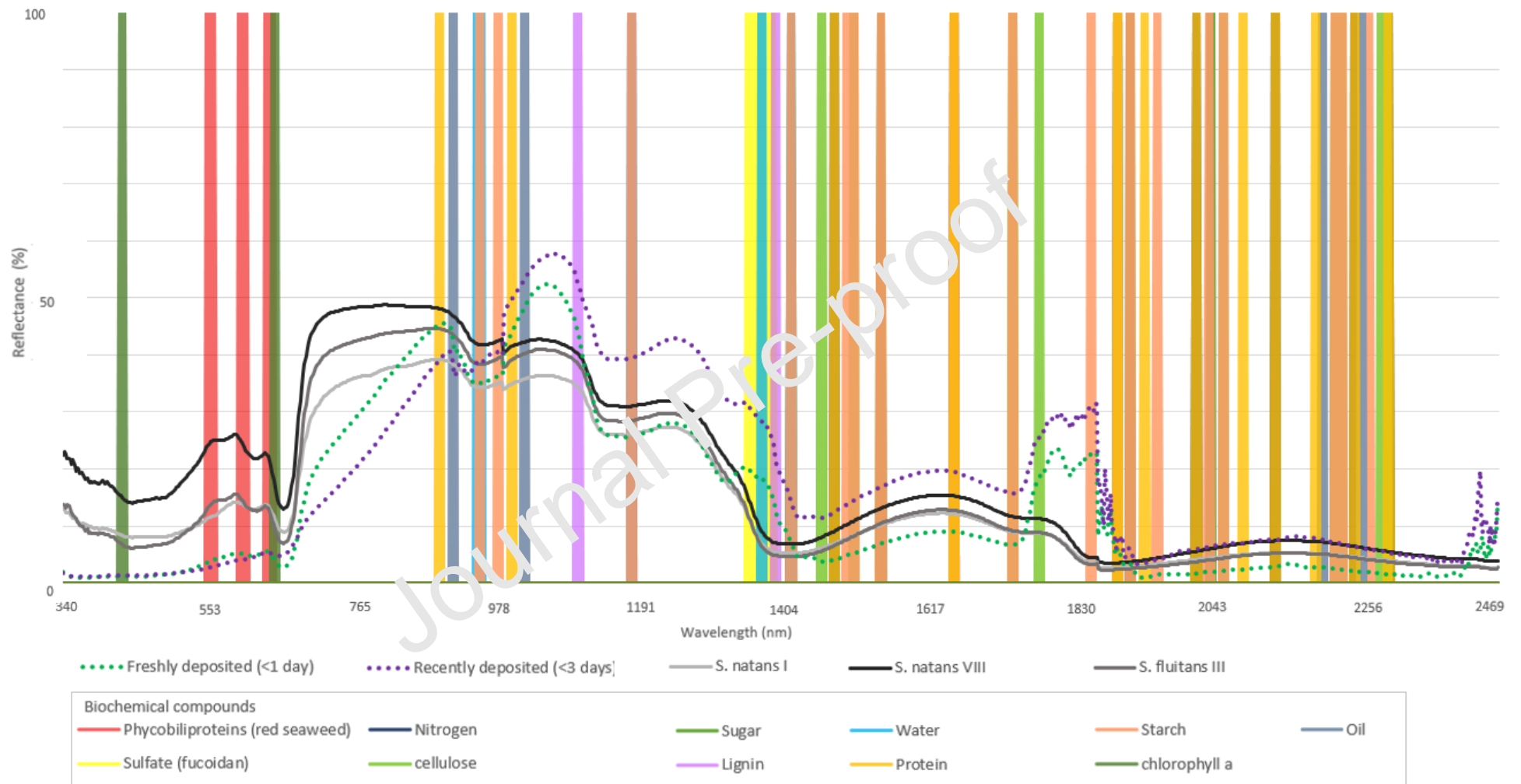
Figure 10 Biochemical analysis. The species and decomposition spectra are plotted with wavelength regions where we can expect to observe specific chemicals. The wavelengths that indicate biochemical compounds were established from literature including Curran (1989), Machado et al. (2022), Agatonovi-Krustin et al. (2020) and Shalev et al. (2022).

27

4. Conclusions

Utilising ground and airborne datasets, we have developed an operational framework for quantifying spectral measurements of pelagic sargassum alongside generating spectral profiles of species/morphotypes, creating decomposition maps, and inferring biochemical composition. In the short term, this preliminary research contributes to understanding the spectral properties of sargassum morphotypes and decomposition levels. We presented the first in situ remote assessment of pelagic sargassum on beaches and found that fresh gold and recent brown sargassum are spectrally distinct; sargassum profiles have a distinct absorption feature between 920 nm and 1080 nm; signals for water and other chemical compounds suggest that different morphotypes and decomposition levels contain differing quantities which has implications for use. The method developed could be used to easily determine the quality of beached sargassum to inform harvesting and processing of the biomass and could replace the current costly requirement of collecting, drying, and transporting samples to a laboratory to determine their value. In the longer term, we expect utilising remote sensing and spectroscopy capabilities in combination with biochemical techniques to allow for better monitoring of pelagic sargassum from air and space borne methods, as well as the opportunity for quality assessments for commercial harvesting and valorisation. This would support management of this environmental challenge by providing crucial information for utilising pelagic sargassum.

In areas where sargassum cannot be monitored remotely due to weather and cloud cover conditions, this approach to data collection issues could provide simpler methods of sargassum quality and quantity assessment. While any in situ monitoring requires people to undertake the monitoring, there are emerging approaches to gather such data. Some of the outstanding challenges, could be addressed through utilising citizen science methods and engaging communities affected by sargassum in research. Reflectance analysis could be used to explore seasonal and

annual variation as well. In line with this, we noted a variation in spectral profiles collected at each location, and we attributed this to the field conditions and consequent variation in methods we employed. However, in future research, it would be valuable to explore if variation in biochemical composition also contributed to the differing spectra. Integrating interdisciplinary methods from biology and remote sensing would facilitate impactful research to advance knowledge on detection, migration, and biology of pelagic sargassum.

References

Agatonovic-Kustrin, S., Ramenskaya, G., Kustrin, E., Ortakand, D.B. and Morton, D.W., 2020. A new integrated HPTLC-ATR/FTIR approach in marine algae bioprofiling. Journal of Pharmaceutical and Biomedical Analysis, 189, p.113488.

Alleyne, K.S., Neat, F. and Oxenford, H.A., 2023. A baseline assessment of the epiphytic community associated with pelagic sargassum in the Tropical Atlantic. Aquatic Botany, 186, p.103635.

ANSES 2017 French Agency for Food, Environmental and Occupational Health & Safety (in French) https://www.anses.fr/en/system/files/AIR2015SA0225Ra.pdf

Arellano-Verdejo, J., Lazcano-Hernandez, H.E. and Cabanillas-Terán, N., 2019. ERISNet: deep neural network for Sargassum detection along the coastline of the Mexican Caribbean. PeerJ, 7, p.e6842.

Asner, G.P., Martin, R.E., Anderson, C.B. and Knapp, D.E., 2015. Quantifying forest canopy traits: Imaging spectroscopy versus field survey. Remote Sensing of Environment, 158, pp.15-27.

Baldwin, K., Oxenford, H., Weeked, J., Small, M., Irvine, J., Desai, A. 2022. Monitoring Protocol Drones. SargAdapt Good Practice Guide Series. Volume 1. [URL: https://www.cavehill.uwi.edu/ cermes/projects/sargassum/docs/tools/smp_vol_01_drones_june_2022.aspx]

Bian, M., Skidmore, A.K., Schlerf, M., Wang, T., Liu, Y., Zeng, R. and Fei, T., 2013. Predicting foliar biochemistry of tea (*Camellia sinensis*) using reflectance spectra measured at powder, leaf and canopy levels. ISPRS Journal of Photogrammetry and Remote Sensing, 78, pp.148-156.

Brach, M., Chan, J. W., & Szymanski, P. (2019). Accuracy assessment of different photogrammetric software for processing data from low-cost UAV platforms in forest conditions. iForest-Biogeosciences and Forestry, 12(5), 435.

Burggraaff, O., Schmidt, N., Zamorano, J., Pauly, K., Pascual, S., Tapia, C., Spyrakos, E. and Snik, F., 2019. Standardized spectral and radiometric calibration of consumer cameras. Optics express, 27(14), pp.19075-19101.

Casal, G., Kutser, T., Domínguez-Gómez, J.A., Sánchez-Carnero, N. and Freire, J., 2013. Assessment of the hyperspectral sensor CASI-2 for macroalgal discrimination on the Ría de Vigo coast (NW Spain) using field spectroscopy and modelled spectral libraries. Continental Shelf Research, 55, pp.129-140.

Chávez, V., Uribe-Martínez, A., Cuevas, E., Rodríguez-Martínez, R.E., Van Tussenbroek, B.I., Francisco, V., Estévez, M., Celis, L.B., Monroy-Velázquez, L.V., Leal-Bautista, I. and Álvarez-Filip, L., 2020. Massive influx of pelagic Sargassum spp. on the coasts of the Mexican Caribbean 2014–2020: challenges and opportunities. Water, 12(10), p.2908.

Congedo, L., 2021. Semi-Automatic Classification Plugin: A Python tool for the download and processing of remote sensing images in QGIS. Journal of Open Source Software, 6(64), 3172, https://doi.org/10.21105/joss.03172

Curran, P.J., 1989. Remote sensing of foliar chemistry. Remote sensing of environment, 30(3), pp.271-278.

Davis, D., Simister, R., Campbell, S., Marston, M., Bose, S., McQueen-Mason, S.J., Gomez, L.D., Gallimore, W.A. and Tonon, T., 2021. Biomass composition of the golden tide pelagic seaweeds *Sargassum fluitans* and *S. natans* (morphotypes I and VIII) to inform valorisation pathways. Science of the Total Environment, 762, p.143134.

de la Barreda-Bautista, B., Metcalfe, S.E., Smith, G., Sjögersten, S., Boyd, D.S., Cerdeira-Estrada, S., López-Ramírez, P., Magaldi, A., Ressl, R., Perera-Valderrama, S. and Caballero-Aragón, H., 2023. Monitoring holopelagic Sargassum spp. along the Mexican Caribbean coast: understanding and addressing user requirements for satellite remote sensing. Frontiers in Marine Science, 10, p.1166000.

Desrochers A, Cox S-A, Oxenford HA, van Tussenbroek, BI., 2022. Pelagic sargassum: A guide to current and potential uses in the Caribbean. FAO Fisheries and Aquaculture Technical Paper 686, pp. 124, Rome, FAO. https://doi.org/10.4060/cc3147en

Dierssen, H.M., A. Chlus, and B. Russell. 2015. 'Hyperspectral Discrimination of Floating Mats of Seagrass Wrack and the Macroalgae Sargassum in Coastal Waters of Greater Florida Bay Using Airborne Remote Sensing'. Remote Sensing of Environment 167 (September): 247–58. https://doi.org/10.1016/j.rse.2015.01.027.

Diruit, W., Le Bris, A., Bajjouk, T., Richier, S., Helias, M., Burel, T., Lennon, M., Guyot, A. and Ar Gall, E., 2022. Seaweed habitats on the shore: Characterization through hyperspectral UAV imagery and field sampling. Remote Sensing, 14(13), p.3124.

Féret, J.B. and Asner, G.P., 2014. Mapping tropical forest canopy diversity using high-fidelity imaging spectroscopy. Ecological Applications, 24(6), pp.1283-1296.

Fidai, Y.A., Dash, J., Tompkins, E.L. and Tonon, T., 2020. A systematic review of floating and beach landing records of Sargassum beyond the Sargasso Sea. Environmental Research Communications, 2(12), p.122001.

Gamon, J.A., Rahman, A.F., Dungan, J.L., Schildhauer, M. and Huemmrich, K.F., 2006. Spectral Network (SpecNet)—What is it and why do we need it?. Remote Sensing of Environment, 103(3), pp.227-235.

Gao, Z., Xu, F., Shang, W., Jiang, X., Song, D. and Chen, M., 2018, September. Estimating initial biomass of green tide algae in the South Yellow Sea with aid of UAV and S2A data. In Remote Sensing and Modeling of Ecosystems for Sustainability XV (Vol. 10767, pp. 232-236). SPIE.

García-Sánchez, M., Graham, C., Vera, E., Escalante-Mancera, E., Álvarez-Filip, L. and van Tussenbroek, B.I., 2020. Temporal changes in the composition and biomass of beached pelagic Sargassum species in the Mexican Caribbean. Aquatic Botany, 167, p.103275.

Guiry, M.D. and Guiry, G.M., 2023. *AlgaeBase*. World-wide electronic publication, National University of Ireland, Galway. https://www.algaebase.org ; searched on 28 February 2023.

Gower, J.F. and King, S.A., 2011. Distribution of floating Sargassum in the Gulf of Mexico and the Atlantic Ocean mapped using MERIS. International Journal of Remote Sensing, 32(7), pp.1917-1929.

Hodgkins, Hagen, Tatyana Matthews, Derek Morris, James Boswell, Andrew Brumfield, Robert Y. George, and Linda Hayden. 2017. 'Quantifying Sargassum Boundaries on Eastern and Western Walls of the Gulf Stream Protruding near Cape Hatteras into Sargasso Sea Bermuda/Azores'. In 2017 IEEE International Geoscience and Remote Sensing Symposium (IGARSS), 2157–70. https://doi.org/10.1109/IGARSS.2017.8127416.

Hu, Chuanmin. 2009. 'A Novel Ocean Color Index to Detect Floating Algae in the Global Oceans'. Remote Sensing of Environment 113 (10): 2118–29. https://doi.org/10.1016/j.rse.2009.05.012.

Hu, Chuanmin, Lian Feng, Robert F. Hardy, and Eric J. Hochberg. 2015. 'Spectral and Spatial Requirements of Remote Measurements of Pelagic Sargassum Macroalgae'. Remote Sensing of Environment 167 (September): 229–46. https://doi.org/10.1016/j.rse.2015.05.022.

Kloc, B., Mazur, A., Szumiło, M. (2021). Comparison of Free and Commercial Software in the Processing of Data Obtained from Non-Metric Cameras. Journal of Ecological Engineering, 22(2), 213-225.

Kokaly, R.F. and Clark, R.N., 1999. Spectroscopic determination of leaf biochemistry using band-depth analysis of absorption features and stepwise multiple linear regression. Remote sensing of environment, 67(3), pp.267-287.

Lazcano-Hernandez, H.E., Arellano-Verdejo, J. and Rodrıguez-Martınez, R.E., 2023. Algorithms applied for monitoring pelagic Sargassum. Frontiers in Marine Science, 10, p.1216426.

León-Pérez, M.C., Reisinger, A.S. and Gibeaut, J.C., 2023. Spatial-temporal dynamics of decaying stages of pelagic Sargassum spp. along shorelines in Puerto Rico using Google Earth Engine. Marine Pollution Bulletin, 188, p.114715.

Machado, C.B., Maddix, G.M., Francis, P., Thomas, S.L., Burton, J.A., Langer, S., Larson, T.R., Marsh, R., Webber, M. and Tonon, T., 2022. Pelagic Sargassum events in Jamaica: Provenance, morphotype abundance, and influence of sample processing on biochemical composition of the biomass. Science of the Total Environment, 817, p.152761.

Malenovský, Z., Homolová, L., Lukeš, P., Buddenbaum, H., Verrelst, J., Alonso, L., Schaepman, M.E., Lauret, N. and Gastellu-Etchegorry, J.P., 2019. Variability and uncertainty challenges in scaling imaging spectroscopy retrievals and validations from leaves up to vegetation canopies. Surveys in Geophysics, 40, pp.631-656.

Mancini, F., Dubbini, M., Gattelli, M., Stecchi, F., Fabbri, S., Gabbianelli, G., (2013). Using unmanned aerial vehicles (UAV) for high-resolution reconstruction of topography: the structure from motion approach on coastal environments. Remote Sens. 5, 6880–6898.

Marmorino, G.O., Miller, W.D., Smith, G.B. and Bowles, J.H., 2011. Airborne imagery of a disintegrating Sargassum drift line. Deep Sea Research Part I: Oceanographic Research Papers, 58(3), pp.316-321.

Maurer, A.S., De Neef, E. and Stapleton, S., 2015. Sargassum accumulation may spell trouble for nesting sea turtles. Frontiers in Ecology and the Environment, 13(7), pp.394-395.

McGlathery, K.J., 2001. Macroalgal blooms contribute to the decline of seagrass in nutrient-enriched coastal waters. Journal of Phycology, 37(4), pp.453-456.

Milledge, J.J., Nielsen, B.V. and Bailey, D., 2016. High-value products from macroalgae: the potential uses of the invasive brown seaweed, *Sargassum muticum*. Reviews in Environmental Science and Bio/Technology, 15, pp.67-88.

Myneni, R.B., Hall, F.G., Sellers, P.J. and Marshak, A.L., 1995. The interpretation of spectral vegetation indexes. IEEE Transactions on Geoscience and remote Sensing, 33(2), pp.481-486.

Nurdin, N., Alevizos, E., Syamsuddin, R., Asis, H., Zainuddin, E.N., Aris, A., Oiry, S., Brunier, G., Komatsu, T. and Barillé, L., 2023. Precision Aquaculture Drone Mapping of the Spatial Distribution of Kappaphycus alvarezii Biomass and Carrageenan. Remote Sensing, 15(14), p.3674.

Ody, A., Thibaut, T., Berline, L., Changeux, T., Andre, J.M., Chevalier, C., Blanfune, A., Blanchot, J., Ruitton, S., Stiger-Pouvreau, V. and Connan, S., 2019. From In Situ to satellite observations of pelagic Sargassum distribution and aggregation in the Tropical North Atlantic Ocean. PLoS One, 14(9), p.e0222584.

Olmedo-Masat, O.M., Raffo, M.P., Rodríguez-Pérez, D., Arijón, M. and Sánchez-Carnero, N., 2020. How far can we classify macroalgae remotely? An example using a new spectral library of species from the south west atlantic (Argentine Patagonia). Remote Sensing, 12(23), p.3870.

Oxenford, H.A., Cox, S.A., van Tussenbroek, B.I. and Desrochers, A., 2021. Challenges of turning the Sargassum crisis into gold: current constraints and implications for the Caribbean. Phycology, 1(1), pp.27-48.

Parr, A.E., 1939. Quantitative observations on the pelagic Sargassum vegetation of the western North Atlantic. Bull. Bingham oceanogr. Coll., 6, pp.1-94.

Ped, J., Scaduto, E., Accorsi, E. and Torres-Pérez, J., 2016. Caribbean Oceans: Utilizing NASA Earth Observations to Detect, Monitor, and Respond to Unprecedented Levels of Sargassum in the Caribbean Sea (No. NF1676L-24244).

Putman, N.F., Beyea, R.T., Iporac, L.A.R., Triñanes, J., Ackerman, E.G., Olascoaga, M.J., Appendini, C.M., Arriaga, J., Collado-Vides, L., Lumpkin, R. and Hu, C., 2023. Improving satellite monitoring of coastal inundations of pelagic Sargassum algae with wind and citizen science data. Aquatic Botany, p.103672.

R Development Core Team. (2021). R: A language and environment for statistical computing.

http://www.r-project.org/

Ramlogan, N.R., McConney, P. and Oxenford, H.A., 2017. Socio-economic impacts of Sargassum

influx events on the fishery sector of Barbados. Centre for Resource Management and

Environmental Studies (CERMES), University of the West Indies: Cave Hill, Barbados, p.86.

Resiere, D., Valentino, R., Nevière, R., Banydeen, R., Gueye, P., Florentin, J., Cabié, A., Lebrun, T.,

Mégarbane, B., Guerrier, G. and Mehdaoui, H., 2018. Sargassum seaweed on Caribbean islands: an

international public health concern. The Lancet, 392(10165), p.2691.

Rhein-Knudsen, N., Ale, M.T., Ajalloueian, F. and Meyer, A.S. 2017. Characterization of alginates

from Ghanaian brown seaweeds: *Sargassum* spp. and *Padina* spp. Food Hydrocolloids, 71, pp.236-

244.

Roca Mora, M., Bonnet, M., Román, A., Caballero, I., Zoffoli, M.L., Gernez, P. and Navarro, G., 2022.

Monitoring the marine invasive alien species *Rugulopteryx okamurae* using unmanned aerial vehicles

and satellites. Frontiers in Marine Science, 9, p.2088.

Rodríguez-Martínez, R.E., Medina-Valmaseda, A.E., Blanchon, P., Monroy-Velázquez, L.V., Almazán-

Becerril, A., Delgado-Pech, B., Vásquez-Yeomans, L., Francisco, V. and García-Rivas, M.C., 2019.

Faunal mortality associated with massive beaching and decomposition of pelagic Sargassum. Marine

Pollution Bulletin, 146, pp.201-205.

Schell, J.M., Goodwin, D.S. and Siuda, A.N., 2015. Recent Sargassum inundation events in the

Caribbean: shipboard observations reveal dominance of a previously rare form. Oceanography,

28(3), pp.8-11.Shalev, N.T., Ghermandi, A., Tchernov, D., Shemesh, E., Israel, A. and Brook, A., 2022.

NIR spectroscopy and artificial neural network for seaweed protein content assessment in-situ.

Computers and Electronics in Agriculture, 201, p.107304.

Small, M., Irvine, J., Baldwin, K., Weekes, J., Oxenford, H.A., 2022. Sargassum Monitoring Protocol Beach. SargAdapt Good Practice Guide Series, Volume 2 [URL: https://www.cavehill.uwi.edu/cermes/projects/sargassum/docs/tools/smp_vol_02_beach_-june_2022.aspx]

Solarin, B.B., Bolaji, D.A., Fakayode, O.S. and Akinnigbagbe, R.O., 2014. Impacts of an invasive seaweed Sargassum hystrix var. fluitans (Børgesen 1914) on the fisheries and other economic implications for the Nigerian coastal waters. IOSR Journal of Agriculture and Veterinary Science, 7(7), pp.1-6.

Su, W.H., 2020. Advanced machine learning in point spectroscopy, RGB-and hyperspectral-imaging for automatic discriminations of crops and weeds: A review. Smart Cities, 3(3), pp.767-792.

Sutton, M., Stum, J., Hajduch, G., Dufau, C., Maréchal, J.P. and Lucas, M., 2019, June. Monitoring a new type of pollution in the Atlantic Ocean: the sargassum algae. In OCEANS 2019-Marseille (pp. 1-4). IEEE.

Szekielda, K.H., Marmorino, G.O., Bowles, J.H. and Gillis, D.B., 2010. High spatial resolution spectrometry of rafting macroalgae (Sargassum). Journal of Applied Remote Sensing, 4(1), p.043529.

Taylor, W.R., 1972. *Marine algae of the eastern tropical and subtropical coasts of the Americas*. University of Michigan.

Valentini, N. and Balouin, Y., 2020. Assessment of a smartphone-based camera system for coastal image segmentation and sargassum monitoring. Journal of Marine Science and Engineering, 8(1), p.23.

van Tussenbroek, B.I.; Hernández Arana, H.A.; Rodríguez-Martínez, R.E.; Espinoza-Avalos, J.; Canizales-Flores, H.M.; GonzálezGodoy, E.; Barba-Santos, M.G.; Vega-Zepeda, A.; Collado-Vides, L. 2017. Severe impacts of brown tides caused by Sargassum spp. on near-shore Caribbean seagrass communities. Marine pollution bulletin, 122(1-2), pp.272-281.

Wang, M., Hu, C., Barnes, B.B., Mitchum, G., Lapointe, B. and Montoya, J.P., 2019. The great Atlantic sargassum belt. Science, 365(6448), pp.83-87.

Webster, R.K. and Linton, T., 2013. Development and implementation of Sargassum early advisory system (SEAS). Shore & Beach, 81(3), p.1.

Wu, D., Li, R., Zhang, F. and Liu, J., 2019. A review on drone-based harmful algae blooms monitoring. Environmental monitoring and assessment, 191, pp.1-11.

Xu, F., Gao, Z., Jiang, X., Shang, W., Ning, J., Song, D. and Ai, J., 2018. UAV and S2A data-based estimation of the initial biomass of green algae in the South Yellow Sea. Marine pollution bulletin, 128, pp.408-414.

Author Contribution Statement:

Yanna Alexia Fidai: data curation, formal analysis, investigation, methodology, roles/writing – original draft
Carla Machado: formal analysis, writing – review/editing
Victoria Dominguez Almela: formal analysis, writing – review/editing
Hazel Oxenford: data curation, writing – review/editing
Philip-Neri Jayson-Quashigah: data curation, writing – review/editing
Thierry Tonon: data curation, supervision, writing – review/editing
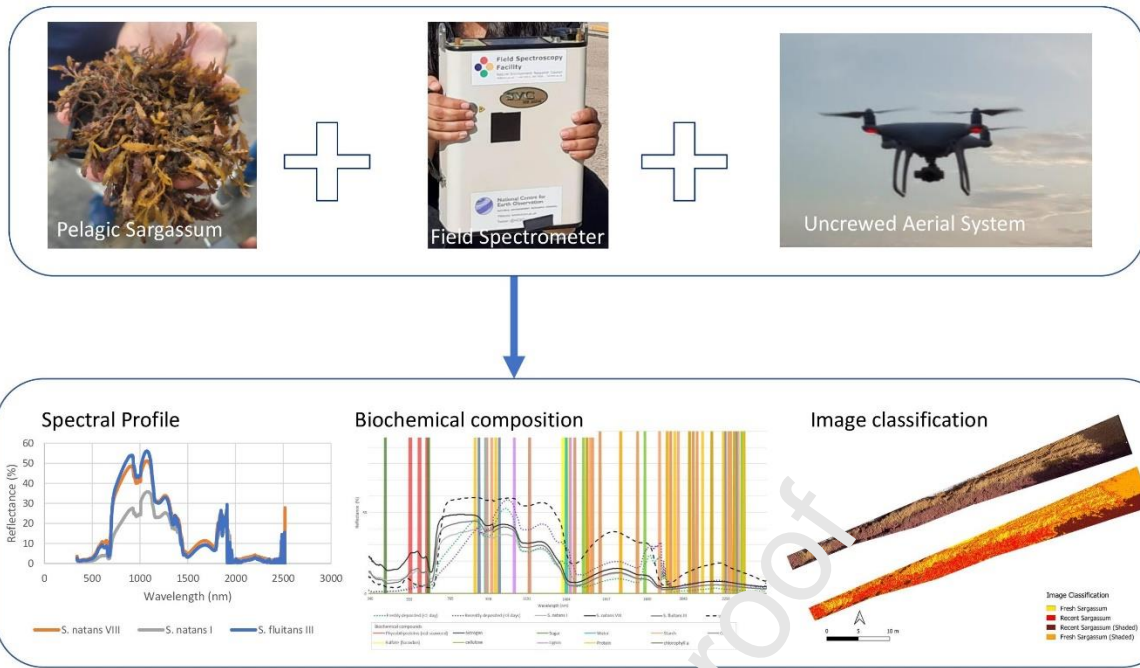Jadu Dash: conceptualisation, data curation, supervision, writing – review/editing

Declaration of interests

☒ The authors declare that they have no known competing financial interests or personal relationships that could have appeared to influence the work reported in this paper.

☐ The authors declare the following financial interests/personal relationships which may be considered as potential competing interests:

Graphical abstract

Highlights:

42

- New operational framework to detect beached pelagic sargassum.
- Spectral and airborne data from sargassum beaching events in Barbados and Ghana.
- Spectral profiles of three morphotypes and fresh and old beached sargassum.
- Fresh and old sargassum are spectrally distinct.
- Estimation of biochemical composition of pelagic sargassum from spectra.